

Low-Loss Single-Material Fibers Made From Pure Fused Silica

By P. KAISER and H. W. ASTLE

(Manuscript received January 22, 1974)

Low-loss single- and multimode optical fibers were fabricated solely from pure fused silica. Their spectral losses corresponded closely to those of unclad fibers drawn from the same material, provided the cores of the single-material fiber preform were redrawn under pure conditions. The lowest steady-state loss of about 3 dB/km at a wavelength of 1.1 μm was obtained with a fiber 130 meters long that had a Spectrosil WF core. Experimental numerical apertures agreed excellently with theoretical predictions.

I. INTRODUCTION

Recently, we introduced an optical fiber that utilizes only a single, low-loss material in a unique structural form.¹ In the single-material fiber, the light is guided in a core of arbitrary shape which is supported by spoke-like membranes within a protective tubing. The guided modes have exponentially decaying fields in the supporting slabs, so that for proper design no power is lost to the surrounding tube. For a slab of arbitrary thickness, single- and multimode operation can be obtained by choosing the proper size of the central core region. In practice, though, this thickness cannot be too large if the field amplitude is to be sufficiently small at the end of the slabs to result in a fiber of reasonable size.

Theoretical analysis of the single-material fiber has been carried out and is presented in Refs. 2 and 3. In this paper, we concentrate on the experimental evaluation of the transmission characteristic and bring only a summary of those theoretical results that help us to understand the experimental data.

Cross-sectional views of typical single- and multimode fibers are shown in Fig. 1. For a unitary aspect ratio, $h = w$, the rectangular

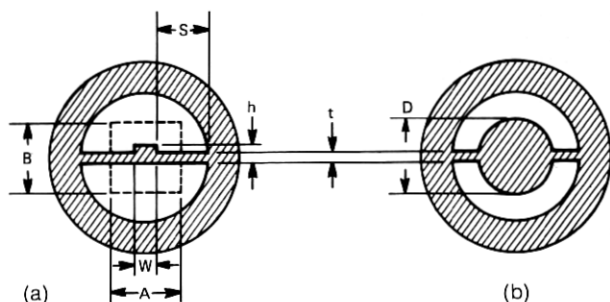


Fig. 1—Cross-sectional views of rectangular and cylindrical core, single-mode ($w \times h$) and multimode ($A \times B$; D) single-material fibers.

core of Fig. 1a has single-mode propagation if the condition

$$h \leq 2t \quad (1)$$

is satisfied.² This result is based on the assumption that the energy is primarily concentrated in the dielectric, and that wavelength λ is small compared to the slab thickness t :

$$\lambda \ll t. \quad (2)$$

For a multimode guide, the wave propagation effects of the slab support can be represented by a uniform-index side support having the same height as the core and an equivalent index $n_e = n(1 - \Delta)$, where n is the refractive index of the core and Δ is computed from

$$\Delta = \frac{1}{8} \left(\frac{\lambda}{tn} \right)^2. \quad (3)$$

For a given n and λ , the relative refractive-index difference Δ depends only on slab thickness. From Δ , we obtain the numerical aperture (NA) and the modal dispersion, τ ,

$$NA = n\sqrt{2\Delta} = \frac{\lambda}{2t} \quad (4)$$

and

$$\tau = \frac{L}{c} n\Delta, \quad (5)$$

where L is the length of the fiber, and c is the velocity of light in free space. The number of modes N for a core of diameter D (Fig. 1) is approximately given by

$$N \cong \frac{\pi^2}{8} \left(\frac{D}{t} \right)^2. \quad (6)$$

For all guided modes, the field decays exponentially along the slab. The field penetration is the largest for the highest-order mode and decays by $1/e$ in a length l , where

$$l \cong \frac{t}{\pi} \quad (7)$$

provided that h and w are large compared to t .

II. FABRICATION OF SINGLE-MATERIAL FIBERS

The preforms from which single-material fibers were drawn typically consisted of a core rod, a thin, polished plate, and a surrounding thick-walled cladding tube* (Fig. 2). Whereas high-grade synthetic silicas were used for core and plate, commercial-grade fused quartz was satisfactory for the cladding tube. The core rods were drawn from about 7-mm-diameter drawn or polished rods just before assembling the single-material fiber preform. To avoid contaminating these rods, a CO₂ laser or an oxy-hydrogen torch of high purity had to be employed for the redraw operation. Copper, with an associated broad absorption band centered between 0.8 and 0.9 μm , was considered the predominant contaminant in less pure systems.

The core rods were either centered in the cladding tube by means of a capillary tube, as indicated in Fig. 2, or they were attached to the top end of the plates with high-temperature cement. Support plates up to 15 cm long were cut from about 0.1-mm-thick polished plates to fit into the approximately 6.5-mm interior diameter of the cladding tubes (10 mm o.d.). The plates and the inner surface of the cladding tubes were cleaned with acetone and hydrofluoric acid and subsequently rinsed with deionized water. The assembled preform was lowered through a moderately hot oxy-hydrogen torch while helium was blown through the tube to carry away residual contaminants evaporating from the surfaces of the preform elements. The same gas was also used as protective atmosphere during the drawing operation. The fibers were drawn with an oxy-hydrogen ring-burner with an approximate draw-down ratio of 100 to 1. The preform geometry was essentially maintained in the drawn fiber, provided we used a proper drawing temperature. Temperatures that were too high caused the tube to collapse or resulted in slabs that were too short to enable low-loss guidance. Temperatures too low, on the other hand, resulted in

* For simplicity, the outer supporting cylinder is referred to as the cladding tube in the remainder of the text; its different meaning from the cladding of the conventional fiber should be kept in mind.

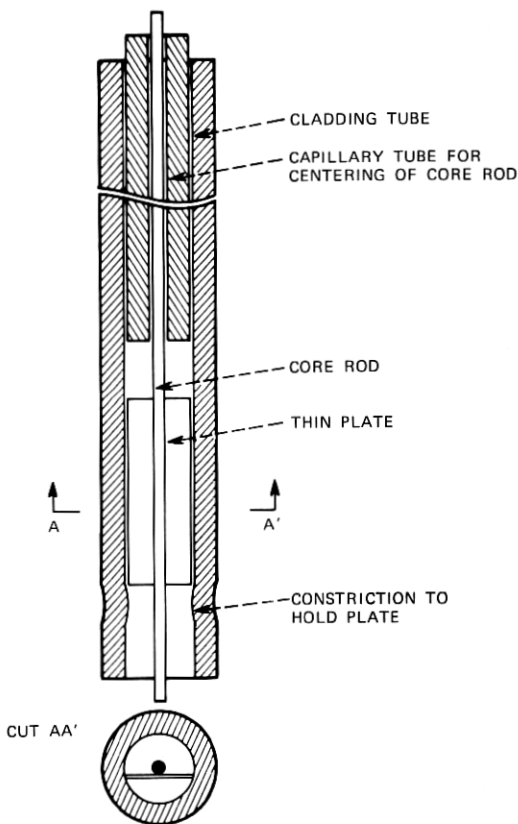


Fig. 2—Preform for single-material fibers.

brittle fibers. Since the core rod is thermally insulated from the heated cladding tube, the maximum diameter of the core rods that could be drawn without difficulty was about 1.5 mm. To avoid collapse of the cladding tube because of excessive heating, a wall thickness of about 1.7 mm was selected. This heavy wall thickness also helped to prevent the tube from being excessively deformed by the surface tension of the slab during the drawing process. Nevertheless, single-mode fibers typically have an elliptical cross section because of this force.

III. SINGLE-MODE, SINGLE-MATERIAL FIBERS

The single-mode fiber shown in Fig. 3 was drawn from an unclad fiber approximately 0.2 mm in diameter and a support plate 0.18 mm thick. The fiber had a slab thickness of $4 \mu\text{m}$, a total core height h of

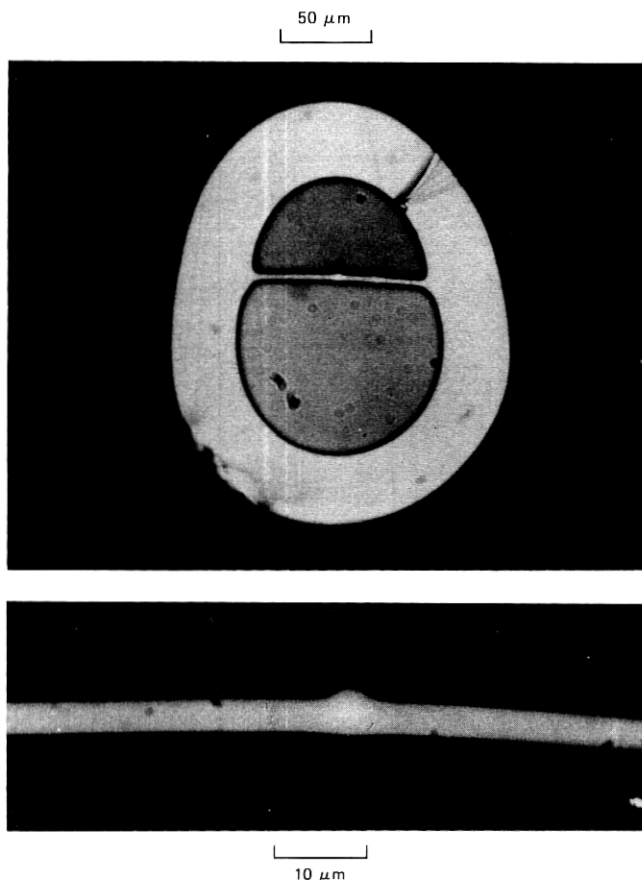


Fig. 3—Cross-sectional picture of single-mode, single-material fiber.

$6 \mu\text{m}$, and an approximate width w of $5 \mu\text{m}$. According to eq. (1), single-mode operation was to be expected. While excited with a HeNe laser at $0.6328 \mu\text{m}$, the intensity distribution of the guided wave was measured by projecting the field distribution of the fiber end with a 40X microscope objective lens to a distant target with a pinhole recording system (Fig. 4). For larger distances from the core region, the intensity in the direction of the slab ($y - y'$) decreases exponentially with a $1/e$ length of $2.3 \mu\text{m}$. As shown in Fig. 4, the intensity distribution in the direction perpendicular to the slab could be well approximated by a $\cos^2 \left(\frac{\pi x}{2 \cdot 3} \right)$ distribution (x in μm). The far-field patterns

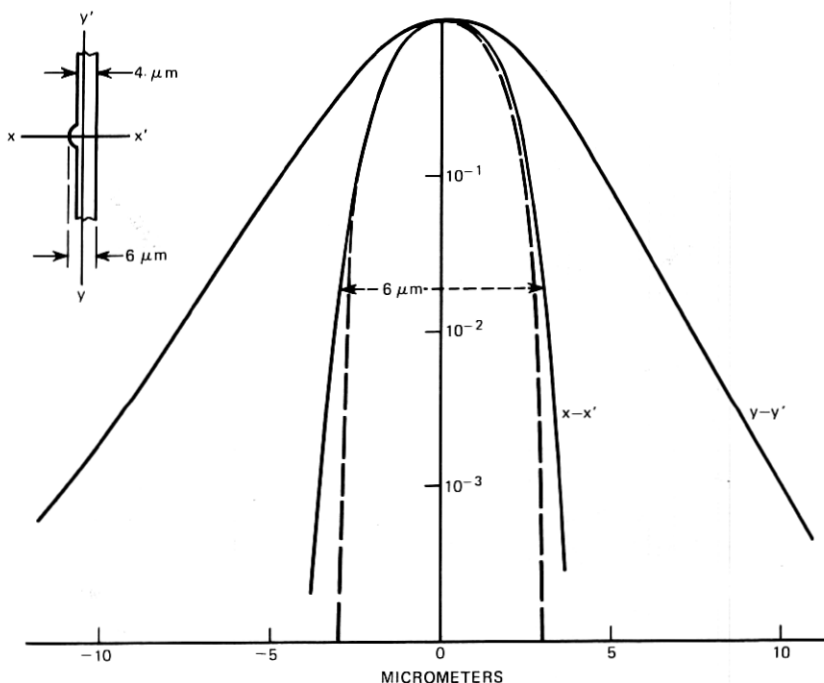


Fig. 4—Near-field intensity of the single-mode, single-material fiber of Fig. 3.

corresponding to this near-field distribution are shown in Fig. 5. These patterns were taken at a distance of 3.4 cm from the fiber end face with a 0.25-mm-diameter pinhole detector. Whereas the broad, exponentially decaying slab field results in a narrow, far-field pattern, the narrow \cos^2 distribution of the perpendicular plane results in a correspondingly broader distribution that has a zero at an angle θ_0 :

$$\sin \theta_0 = \frac{3}{2} \frac{\lambda}{h_{\text{eff}}} \quad (8)$$

with h_{eff} being the effective height of the near-field distribution. With an experimental θ_0 of 11.7 degrees, h_{eff} is computed to be $4.7 \mu\text{m}$, which emphasizes that a substantial part of the energy is propagating in the $4\text{-}\mu\text{m}$ -thick slab.

In addition to this usefully guided field in the core region, we observe other types of modes via their radiation patterns. These modes are more noticeable when the fiber is shorter (less than about 2 m) and straighter. Slab modes typically had a single intensity maximum

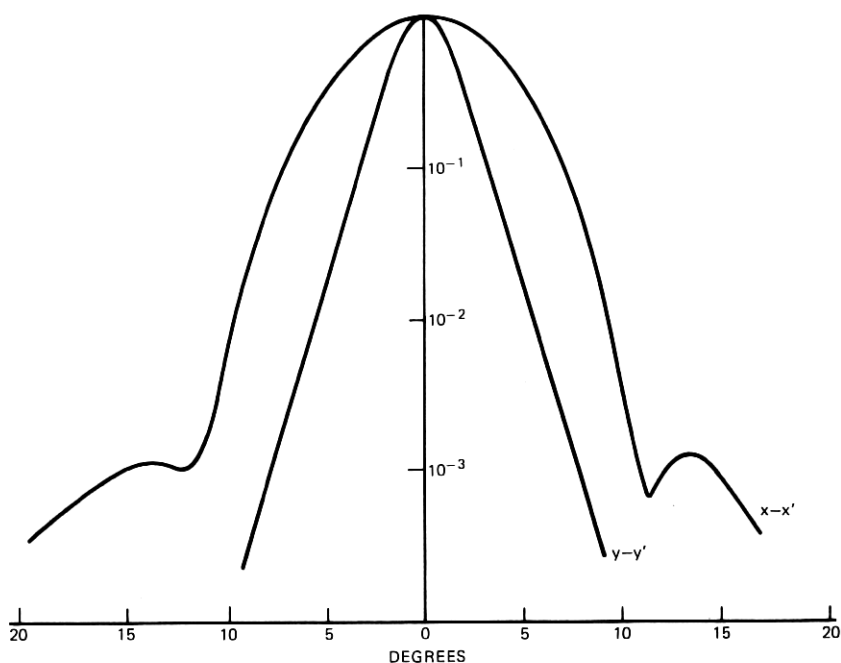


Fig. 5—Far-field intensity of the single-mode, single-material fiber of Figs. 3 and 4.

perpendicular to the slab, and several maxima and minima in the direction of the slab. For guide lengths in the order of a few centimeters, the slab modes are seen to extend to the cladding tube. The first higher mode in the direction perpendicular to the slab could be observed for slab thicknesses in the order of $5 \mu\text{m}$. Besides the rapidly decaying slab modes, we also observed hollow-dielectric waveguide⁴ and cladding modes. Hollow waveguide modes propagating in the voids of the fiber were only excited with low efficiency, and they rapidly decayed within a distance of a few decimeters. For accurate loss measurement, it is important to leave a sufficient length of fiber at the launching end (in excess of 1 m, for example) so that the slab and hollow waveguide modes are sufficiently attenuated. Cladding modes can easily be extracted with a matching liquid.

The single-material fiber losses were measured by breaking off known lengths of fiber and measuring the difference between the power levels. The fibers were broken by scoring them with a diamond while under tension. The fiber end could not be index matched with a liquid to the

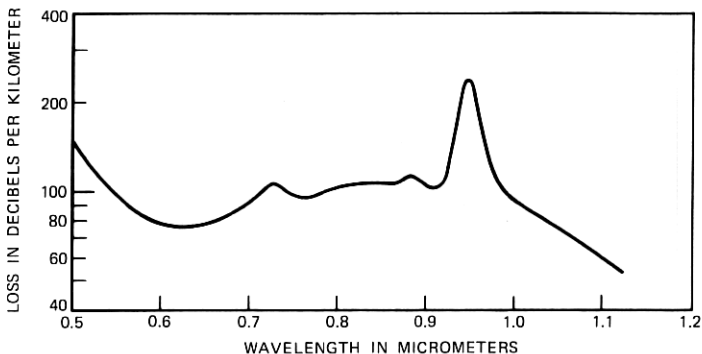


Fig. 6—Spectral losses of a single-mode, single-material fiber made from a Spectrosil WF unclad fiber on a Suprasil 2 plate.

detector surface due to the capillary action exerted by the hollow parts of the fiber. Using a measuring apparatus described elsewhere,⁵ the spectral transmission losses of the single-material fibers were measured between 0.5 and 1.15 μm . Minimum losses achieved with a single-mode, single-material fiber amounted to about 50 dB/km at 1.06 μm (Fig. 6). Despite containing a Spectrosil WF core on a Suprasil 2 plate, the losses of this fiber were comparatively high since the core rod was re-drawn with a low-purity oxy-hydrogen flame. Furthermore, since for

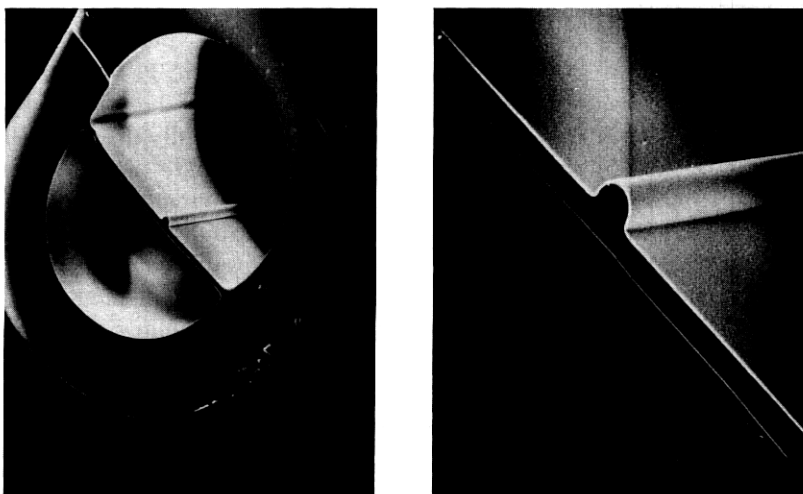


Fig. 7—Electron-microscope pictures of the single-mode, single-material fiber.

single-mode fibers a substantial portion of the energy propagates in the slab, contamination introduced during the polishing process may have contributed to the high losses. Electron-microscope pictures of a single-mode fiber are shown in Fig. 7.

IV. MULTIMODE, SINGLE-MATERIAL FIBERS

Cross-sectional views of multimode, single-material fibers are shown in Figs. 8 and 9. The diameter of the cores typically varied between 20 and 30 μm , depending on the size of the core rod and the draw-down ratio employed. A representative slab thickness was 2 to 3 μm , but fibers with slabs less than 1 μm thick and up to 5 μm thick have also been drawn (Fig. 8). To avoid losses via the exponential tail in the slab, the required minimum length-to-thickness ratio needed to be larger than about a factor of 7. Electron-microscope pictures of the interior structure of a multimode, single-material fiber (Fig. 10) demonstrated the intimate fusion of the preform parts.

The NAs of the multimode, single-material fibers were typically determined at 0.6328 μm from the diameters of the radiation patterns obtained from fibers that were a few meters long. In Fig. 11, the NAs of numerous single-material fibers that vary between 0.07 and 0.32 are compared with theoretical predictions [eq. (4)] and excellent agreement is realized. Diffraction effects made a determination of the NA difficult only for thicker slabs and resulting NAs below about 0.07. It

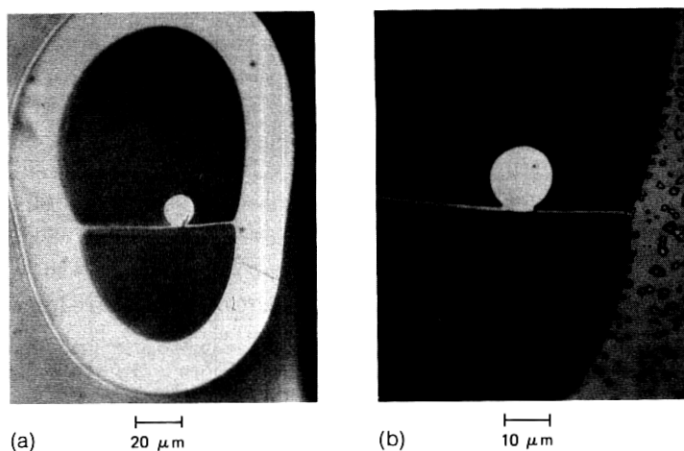


Fig. 8—(a) Cross section of a large-numerical-aperture, multimode fiber with 1- μm -thick supporting slab. ($\text{NA}_{0.6328 \mu\text{m}} = 0.32$.) (b) Magnified core region.

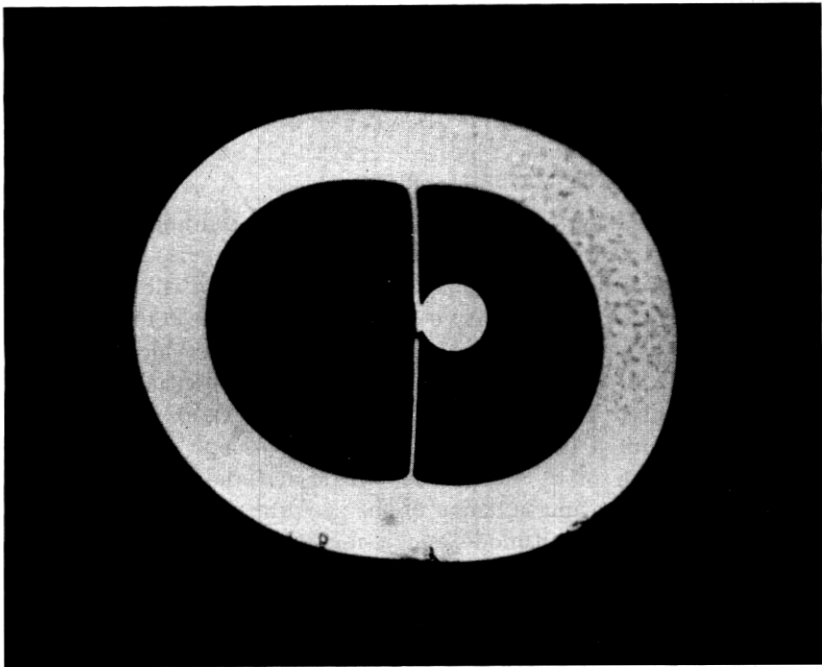


Fig. 9—Cross section of multimode fiber SMF 56 with a Spectrosil WF core on a Suprasil W1 slab ; core diameter $\cong 25 \mu\text{m}$, slab thickness $\cong 2.2 \mu\text{m}$, $\text{NA}_{0.6328 \mu\text{m}} \cong 0.14$.

is noteworthy that the good agreement between theory and experiment enabled us to determine the slab thickness through NA measurements derived from the transmitted radiation pattern. The linear increase of the NA with wavelength also agrees with theory, as illustrated in Fig. 12. Here, a fiber whose NA corresponding to a 2- μm -thick slab was 0.16 at 0.6328 μm , was illuminated by 10-nm bands filtered from a xenon arc lamp,⁵ and the NA was calculated from the 1/100-power-points of the transmitted radiation pattern. Lack of sensitivity limited the data acquisition to the intermediate wavelength region shown, but HeNe-laser measurements at 1.15 μm confirmed a linear dependence in the whole wavelength range investigated.

The transmission losses of single-material fibers were expected to be identical or lower than those of unclad fibers drawn from the same material. Provided that the core rod was drawn in a pure oxy-hydrogen flame, as noted earlier, close agreement was indeed realized (see Fig. 13). Total losses of 10.6 and 10 dB/km were obtained at 0.8 and

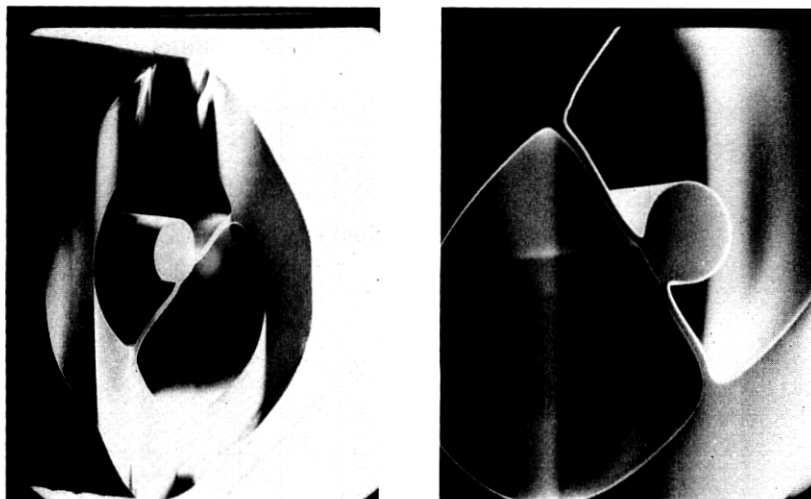


Fig. 10—Electron microscope pictures of a multimode, single-material fiber.

1.06 μm , respectively, with a fiber 210 m long that had a Suprasil 2 core (Fig. 13). The unclad-fiber losses at these wavelengths amounted to 7 and 10.5 dB/km. The various absorption peaks visible in the loss spectrum of Suprasil 2 are, as in Suprasil 1, due to its high OH content of 1200 ppm.⁶ In contrast, only a weak OH band of 3 dB/km appeared in the loss spectrum of a multimode, single-material fiber (SMF 56) with a Spectrosil WF core on a Suprasil W1 slab (Figs. 9 and 14). The approximate steady-state losses of this 130-m-long fiber remained below the 7.5 dB/km level from 0.75 μm to the end of the spectral range investigated, and amounted to 6, 4.5, and 3 dB/km at 0.8, 0.9, and 1.1 μm , respectively.

Approximate steady-state losses were obtained by launching beams with different NAs into the fiber and by measuring the far- and near-end radiation patterns as a function of the launch NA, in addition to the wavelength-dependent transmission losses.⁷ The losses associated with that NA for which the radiation pattern changed least from one end to the other can be considered as the steady-state losses. The radiation patterns were measured at a wavelength of 0.88 μm , which coincides with a resonance peak of the xenon arc lamp. At this wavelength, the 1/100-power-point-equivalent NA was 0.2, which agrees with the theoretical NA and corresponds to that of a 2.2- μm -thick slab. Whereas the NA of single-material fibers increased with wavelength, the NA

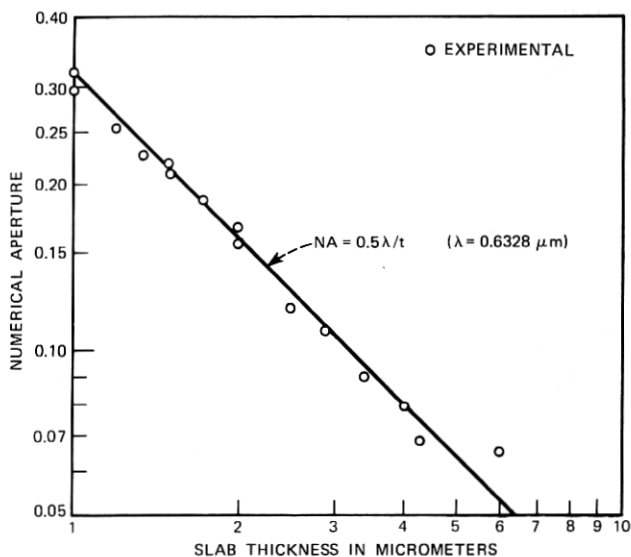


Fig. 11—Numerical aperture as function of slab thickness for multimode, single-material fibers.

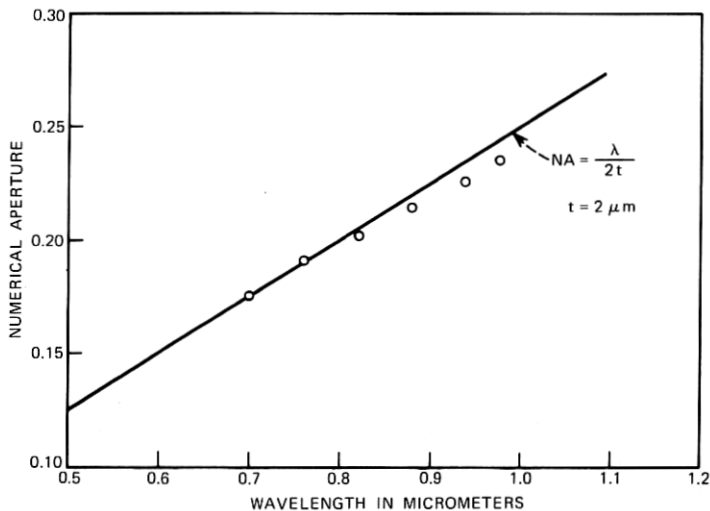


Fig. 12—Numerical aperture as function of wavelength for a multimode, single-material fiber.

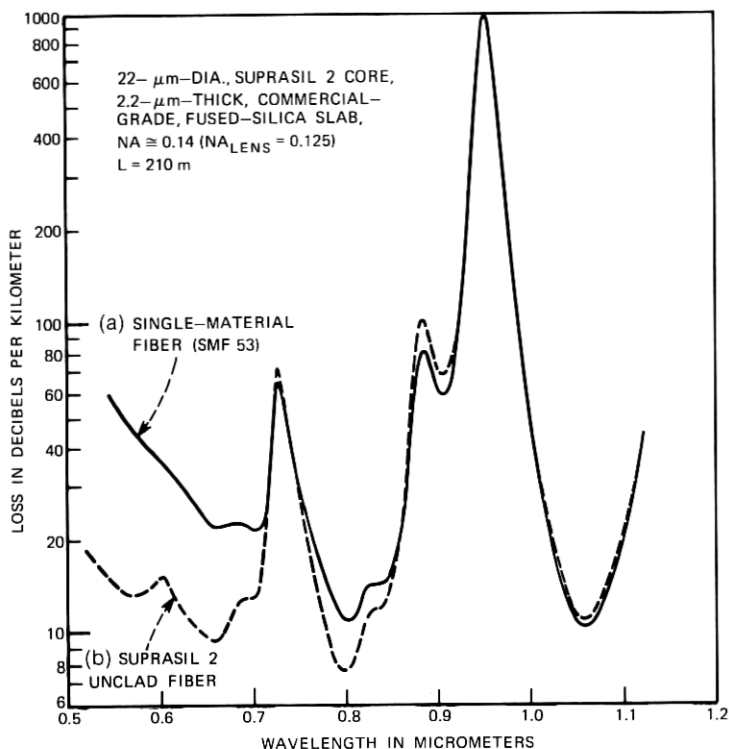


Fig. 13—Spectral losses of a Suprasil 2-cored, single-material fiber compared with unclad fiber losses. (a) Single-material fiber with 22- μm -diameter core and 2.2- μm -slab thickness, $L = 210$ m. (b) Suprasil 2 unclad fiber with approximately 0.2 mm dia; $L \approx 60$ m.

of the launching beam was kept constant during a wavelength scan. Hence, the data obtained are increasingly too high at shorter wavelengths and too low at longer wavelengths relative to the steady-state losses at those wavelengths. We can get an estimate of the possible error by injecting a beam with a small NA into the fiber. The resulting losses are shown as curve b in Fig. 14. Even lower losses were achieved when we cooled the aluminum drum on which the fiber was wound with dry ice to reduce stress-induced losses (Fig. 14, curve c).⁸ With the new minimum losses at 0.8, 0.9, and 1.1 μm amounting to 4, 3.4, and 2.6 dB/km, respectively, this curve represents the lowest loss spectrum obtained for pure fused silica, and corresponds closely to the spectra of the lowest-loss Corning fibers.⁹

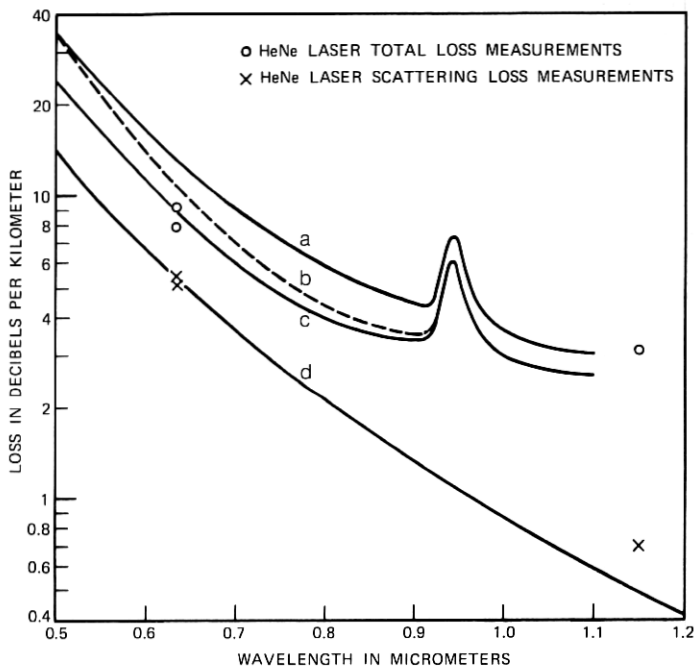


Fig. 14—Spectral losses of multimode fiber SMF 56 with Spectrosil WF core on a Suprasil W1 slab; $L = 130$ m. (a) Approximate steady-state losses. (b) Losses for small-angle excitation. (c) Same as (b) but after stress was relieved by cooling the drum. (d) Rayleigh scattering losses of bulk fused silica.

Total losses of 9 and 3.1 dB/km measured with HeNe lasers at 0.6328 and 1.15 μm agree well with the incoherent-source losses. A 7.8-dB/km loss was obtained at 0.6328 μm for low-order-mode laser excitation. Since scattering losses for this excitation condition amounted to 5.1 dB/km, the approximate absorption losses at 0.6328 μm were 2.7 dB/km. With the scattering losses at 1.15 μm amounting to 0.7 dB/km, the absorption losses there were 2.4 dB/km. The absorption losses of a different Spectrosil WF bulk sample were measured by Rich¹⁰ to be less than 1.6 dB/km at 1.06 μm .

The scattering losses were measured with a 4-cm-long integrating cell built with silicon photo detectors.¹¹ Highly reproducible data were obtained when cladding mode strippers were provided on both sides of the cell, and when small droplets of matching liquid were deposited on the 4-cm-fiber section in the cell to reradiate the otherwise captured cladding power. Scattering losses of 5.5 dB/km were measured at 0.6328 μm when the fiber was filled with a mode spectrum correspond-

ing to the fiber NA of 0.14. This loss value is lower than that reported for a recent low-loss Corning fiber,⁹ and agrees well with the bulk scattering losses of 5 to 6 dB/km measured for numerous fused silica samples by Tynes.¹² Furthermore, it corresponds closely to a value of 5.4 dB/km that was computed from Rich and Pinnow's 12.4 dB/km loss measured at 0.5145 μm , using a λ^{-4} Rayleigh-scattering dependence (curve d in Fig. 14).¹³ It is noteworthy that particularly at shorter wavelengths SMF 56 has approximately the λ^{-4} dependence of Rayleigh-scattering losses.

Whereas the spectral losses of SMF 56 agree closely with the unclad fiber losses of a different batch of Spectrosil WF¹⁴ (Fig. 15, curve b), the unclad fiber losses of the same raw material from which the core rod of SMF 56 was prepared were relatively high (Fig. 15, curve a). This is attributed to imperfections in the preform rod and accidental contamination of the unclad fiber surface. In contrast to an about 11-dB/km OH peak in the unclad fiber loss curve, the single-material-fiber peak at 0.95 μm was a remarkably low 3 dB/km in spite of the

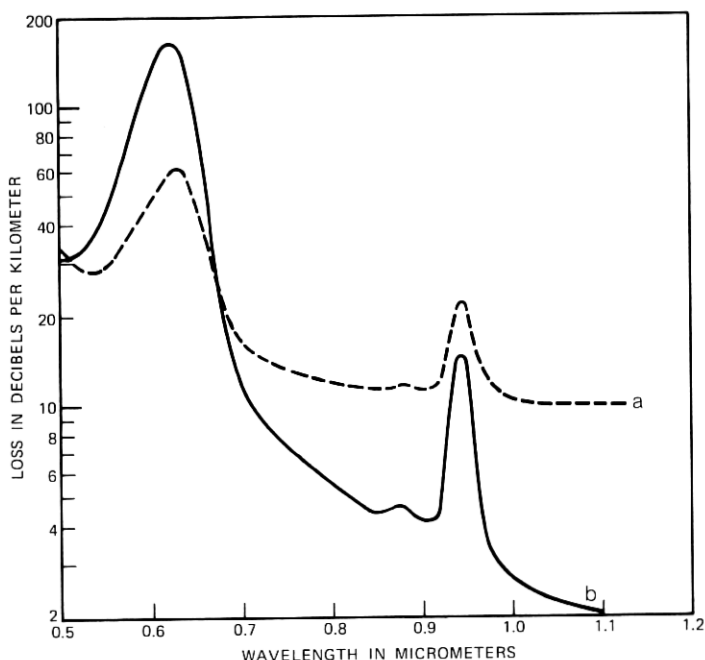


Fig. 15—Loss spectrum of unclad Spectrosil WF fiber. (a) Made from same bulk material as the core of SMF 56. (b) Previously measured sample.

fact that an oxy-hydrogen torch was used for the redraw operation. The difference must be due to the fact that the core rod was only drawn to a diameter of approximately 1.5 mm (compared to the 0.2-mm diameter of the unclad fiber), after which it was surrounded with an inert atmosphere while it was drawn into the single-material fiber. We conclude, therefore, that most of the water in the unclad fiber, and possibly still in the single-material fiber, was introduced in the drawing process, and that the OH content of the raw material could be as low as 1 ppm.⁶

Aside from the water peak at 0.95 μm , the losses of SMF 56 monotonically decreased with wavelength. In contrast, the loss spectra of other single-material and unclad fibers drawn from silica with low OH content exhibit a strong loss band at 0.63 μm .^{6,14,15} Similarly, the 0.63- μm band exists in the unclad fiber drawn from the same raw material (as shown in Fig. 15, curve a), although to a much lesser degree than in other samples evaluated previously. The reason for this is unknown. As shown in Ref. 15, the intensity of the 0.63- μm band depends, among other factors, on the drawing conditions, and it is typically less pronounced in single-material fibers than in related unclad fibers. Also, spontaneous annealing of this band has been observed.

The loss spectrum of a single-material fiber whose Suprasil W1 core was drawn using standard gases and brass fittings, is shown for comparison in Fig. 16. The resulting broad loss band centered between 0.8 and 0.9 μm is believed to be caused by contamination with copper.¹⁶

Preliminary dispersion measurements performed by Cohen¹⁷ with single-material fibers up to 210 m long indicate a weak coupling between modes. The maximum pulse dispersion followed closely the theoretical prediction expressed by eq. (5).

Instead of using the rod-plate technique for the preform preparation, we can achieve longer preform lengths by using thin-walled tubes as supports. A single-mode, single-material fiber created at the intersection of two tubes is shown in Fig. 17.¹⁸ Using three such tubes results in three junctions and associated single-mode guides within the same cladding tube (Fig. 18). Single- and multicore multimode guides using this approach can also be envisioned by supporting one or more core rods by a suitable number of tubes.¹⁹

V. SUMMARY

Low-loss, single- and multimode optical fibers were fabricated solely from pure fused silicas. The single-material fibers consisted of small-diameter rods supported on thin plates in the center of larger-diameter

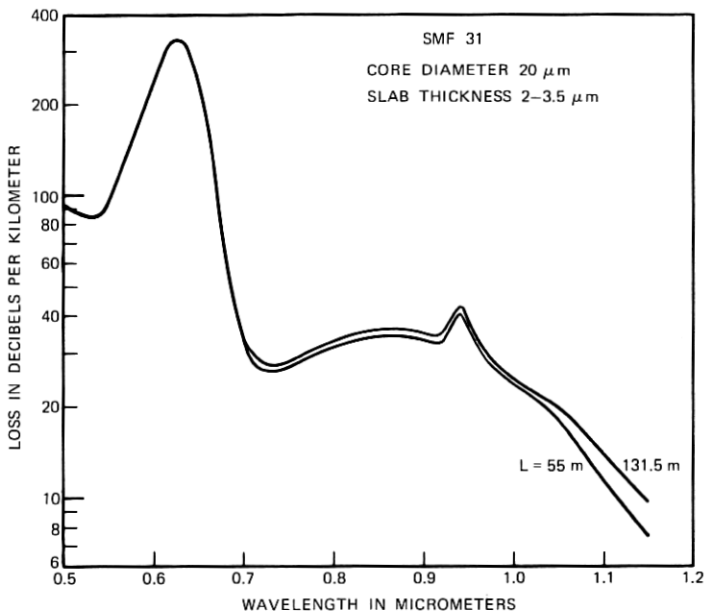
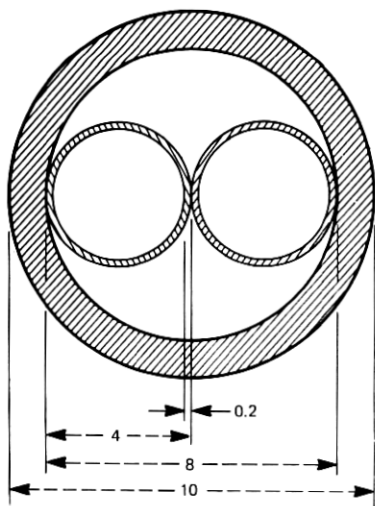


Fig. 16—Spectral losses of a Suprasil W1-cored, single-material fiber whose core was contaminated by an impure flame during the redraw operation.



(a) PREFORM
(DIMENSIONS IN mm)



(b) SINGLE-MODE FIBER SMF 22

Fig. 17—Single-mode, single-material fiber made by fusing two thin-walled tubes.

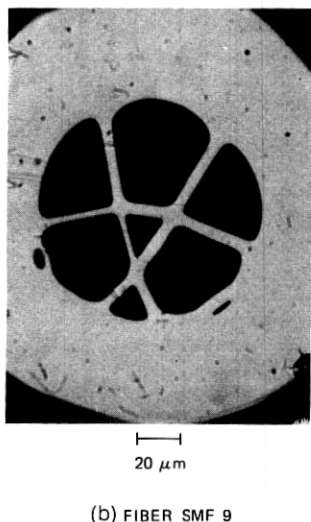
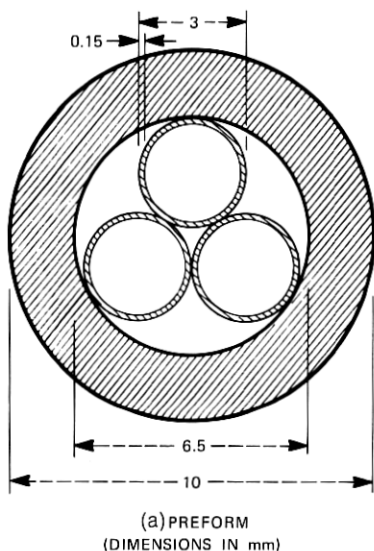


Fig. 18—Multiple-core, single-mode, single-material fiber made by fusing three thin-walled tubes.

protective tubings. The loss spectra of these fibers approached those of unclad fibers drawn from the same raw material. Specifically, steady-state losses of a 130-meter-long multimode fiber with Spectrosil WF core were approximately 6, 4.5, and 3 dB/km at wavelengths of 0.8, 0.9 and 1.1 μm , respectively, with even lower losses existing for low-order mode excitation. Aside from a small 3-dB/km OH band at 0.95 μm , the losses monotonically decreased throughout the 0.5- to 1.15- μm wavelength range investigated. Scattering losses, measured with HeNe lasers at 0.6328 and 1.15 μm , amounted to 5.5 and 0.7 dB/km, respectively.

For supporting plate thicknesses varying between 1 and 4 μm , the experimental NA of multimode fibers changed between 0.32 and 0.08 μm (at 0.6328 μm), which agrees excellently with theoretical predictions. Similarly, the predicted linear increase of the NA with wavelength was confirmed experimentally.

VI. ACKNOWLEDGMENTS

Valuable discussions with and recommendations by E. A. J. Marcanti and S. E. Miller are gratefully acknowledged. We thank A. D. Pearson, W. C. French, and D. D. Bacon for generously making avail-

able their clean-room facilities. R. E. Jaeger's CO₂-laser-drawing assistance, and R. D. Standley's electron-microscope pictures are very much appreciated. S. Gottfried contributed to this paper with some loss measurements of SMF 56.

REFERENCES

1. P. Kaiser, E. A. J. Marcatili, and S. E. Miller, "A New Optical Fiber," *B.S.T.J.*, *52*, No. 2 (February 1973), pp. 265-269.
2. E. A. J. Marcatili, "Slab-Coupled Waveguides," *B.S.T.J.*, *53*, No. 4 (April 1974), pp. 645-674.
3. S. E. Miller, unpublished work.
4. E. A. J. Marcatili and R. A. Schmeltzer, "Hollow Metallic and Dielectric Waveguides for Long Distance Optical Transmission and Lasers," *B.S.T.J.*, *43*, No. 4 (July 1964), pp. 1783-1809.
5. P. Kaiser and H. W. Astle, "Measurement of Spectral Total and Scattering Losses in Unclad Optical Fibers," *J. Opt. Soc. Am.*, *64*, No. 4 (April 1974), pp. 469-474.
6. P. Kaiser et al., "Spectral Losses of Unclad Vitreous Silica and Soda-Lime-Silicate Fibers," *J. Opt. Soc. Am.*, *63*, No. 9 (September 1973), pp. 1141-1148.
7. P. Kaiser, unpublished work.
8. W. B. Gandrud, unpublished work.
9. D. B. Keck, R. D. Maurer, and P. C. Schultz, "On the Ultimate Lower Limit of Attenuation in Glass Optical Waveguides," *Appl. Phys. Lett.*, *22*, No. 7 (April 1973), pp. 307-309. Note also announcement by P. C. Schultz on fabrication of a 2-dB/km fiber at Annual Meeting of American Ceramic Society, Cincinnati, Ohio, April 30-May 2, 1973.
10. T. C. Rich, unpublished work.
11. J. Stone, "Measurement of Rayleigh Scattering in Liquids Using Optical Fibers," *Appl. Opt.*, *12*, No. 8 (August 1973), pp. 1824-1827.
12. A. R. Tynes, unpublished work.
13. D. A. Pinnow, T. C. Rich, F. W. Ostermayer, Jr., and M. DiDomenico, Jr., "Fundamental Optical Attenuation Limits in the Liquid and Glassy State with Application to Fiber Optical Waveguide Materials," *Appl. Phys. Lett.*, *22*, No. 10 (May 1973), pp. 527-529.
14. P. Kaiser, "Spectral Losses of Unclad Fibers Made From High-Grade Vitreous Silica," *Appl. Phys. Lett.*, *23*, No. 1 (July 1973), pp. 45-46.
15. P. Kaiser, "Drawing-Induced Coloration in Vitreous Silica Fibers," *J. Opt. Soc. Am.*, *64*, No. 4 (April 1974), pp. 475-481.
16. H. L. Smith and A. J. Cohen, "Absorption Spectra of Cations in Alkali-Silicate Glasses of High Ultra-Violet Transmission," *Phys. Chem. Glasses*, *4*, No. 5, (October 1963), pp. 173-187.
17. L. G. Cohen, unpublished work.
18. E. A. J. Marcatili, patent filed.
19. P. Kaiser, patent filed.

